Nonchaotic Rayleigh-Bénard Convection with Four and Five Incommensurate Frequencies

R. W. Walden, Paul Kolodner, A. Passner, and C. M. Surko
AT&T Bell Laboratories, Murray Hill, New Jersey 07974
(Received 23 April 1984)

The onset of time dependence of Rayleigh-Bénard convection in water is studied in a rectangular container with aspect ratio 9.5×4.6. Quasiperiodic states are observed exhibiting four and five incommensurate frequencies. All but one of the modes are predominantly localized in different parts of the cell; this localization may explain the coexistence of more than three incommensurate frequencies without chaos.

PACS numbers: 47.25.Qv, 02.50.+s

Much progress has been made in understanding the nonlinear dynamics and the onset of chaos in dissipative systems.[1-5] Consider, for example, Rayleigh-Bénard convection in a horizontal fluid layer heated from below. As the temperature difference across the layer (or the Rayleigh number R) is slowly increased, the steady convective flow first becomes time dependent and then chaotic.[6] In one route to chaos observed in small systems, only two or three modes with incommensurate frequencies are observed before the onset of chaos.[2,4] However, the transition to chaos depends on the nature and strength of the interactions between the modes,[5] and in small systems the interaction between modes is strong. Thus it is unclear what relationship experiments in small systems might have to the onset of chaos in a larger system, where the modes can be more weakly coupled.

In this Letter we report a study of the onset of time dependence in Rayleigh-Bénard convection in a rectangular container of aspect ratio 9.5×4.6. Quasiperiodic states are observed with four and five incommensurate frequencies. Although nonlinear interactions between these modes are observed, most of the modes are found to be predominantly localized in different parts of the cell. These results suggest that spatial localization of the modes can play an important role in determining the route to chaos in an extended system.

The experiments were conducted with water at 50 °C (Prandtl number 3.5) contained in a cell 0.51 cm high with horizontal dimensions 2.32×4.86 cm. The top plate of the cell was sapphire. The cell walls were made of glass, and the bottom plate was copper. Optical access was achieved through an intermediate radiation shield maintained at 50 °C, and the apparatus was enclosed in a vacuum chamber for thermal insulation. A broad, collimated laser beam was directed vertically onto the cell; reflected light from the bottom plate was directed onto a screen, and the image was recorded on video tape. The light intensity was also recorded by a pair of photodiodes (about 1 mm in diameter) which could be positioned anywhere in the image. At each Rayleigh number, data sets of at least 8000 samples were recorded.

As R is increased slowly above the onset, R_c, for steady convective flow, an initial flow pattern is formed with eight horizontal rolls parallel to the short sides of the cell. At $R\simeq10R_c$, the eight parallel rolls have become distorted, and a transition to six rolls is observed via the annihilation of a roll pair in the cell interior. Neither the initial nor the final state is time dependent. The transition occurs at about 60% larger R than predictions of the onset of the skewed-varicose instability assuming infinite aspect ratio.[7] In accord with our observations, a finite aspect ratio would be expected to increase the Rayleigh number of the onset of this instability.

As R is increased further, the six-roll pattern becomes time dependent near $16.2R_c$. These results contrast with observations in much larger cells (e.g., aspect ratio ~30),[8] where time dependence occurs very near the onset of the skewed-varicose instability. These results also contrast with data in much smaller cells, where chaotic behavior occurs without a change in the roll pattern.[2,4]

Above $15R_c$, the state of parallel rolls [shown in Fig. 1(a)] becomes appreciably distorted [Fig. 1(b)]. Then, as R is increased above $16.2R_c$, we observe the successive appearance of four time-dependent modes with incommensurate frequencies—in order of first appearance, $f_1\simeq137$ mHz, $f_2\simeq3$ mHz, $f_3\simeq55$ mHz, and $f_4\simeq124$ mHz. Shown in Figs. 2(a) and 2(b) are frequency spectra measured at different points in the cell. When the intensity is recorded at a location where f_1, f_3, or f_4 is strongest, the power spectrum is completely dominated (by a factor $>10^2$) by that frequency and its harmonics.

Modes f_1, f_3, and f_4 are predominantly localized in different parts of the cell, and the specific location of the modes is different for different distor-

©1984 The American Physical Society

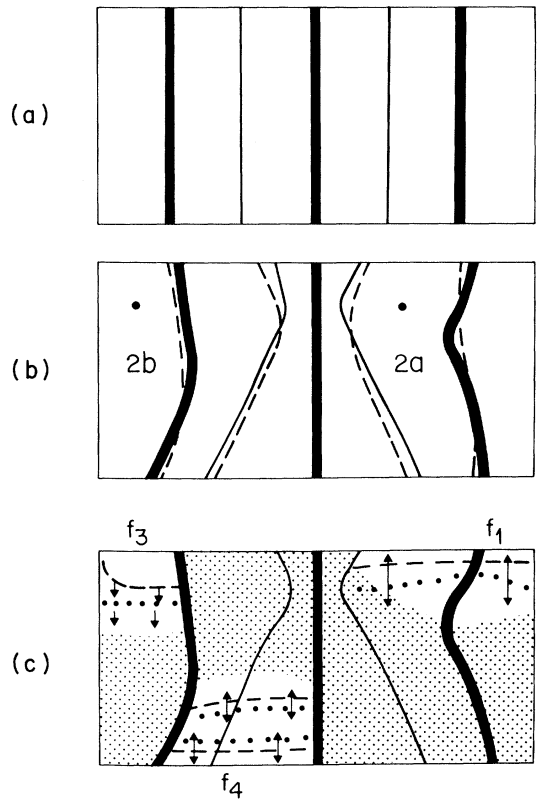

FIG. 1. Schematic representation of the convective flow patterns: (a) Time-independent six-roll pattern observed at $R \lesssim 15R_c$; upflow boundary shown by thin lines and downflow boundary by heavy lines. (b) Distorted and time-dependent pattern at $18.0R_c$; the solid and dashed lines show the positions of the roll boundaries at different phases of the 3-mHz mode, f_2. The dots marked 2(a) and 2(b) refer to Fig. 2. (c) The unshaded areas indicate the regions where modes f_1, f_3, and f_4 are dominant. In these areas, the solid and dashed lines indicate the phase fronts at different parts of a cycle, and the arrows indicate the direction of motion of these phase fronts.

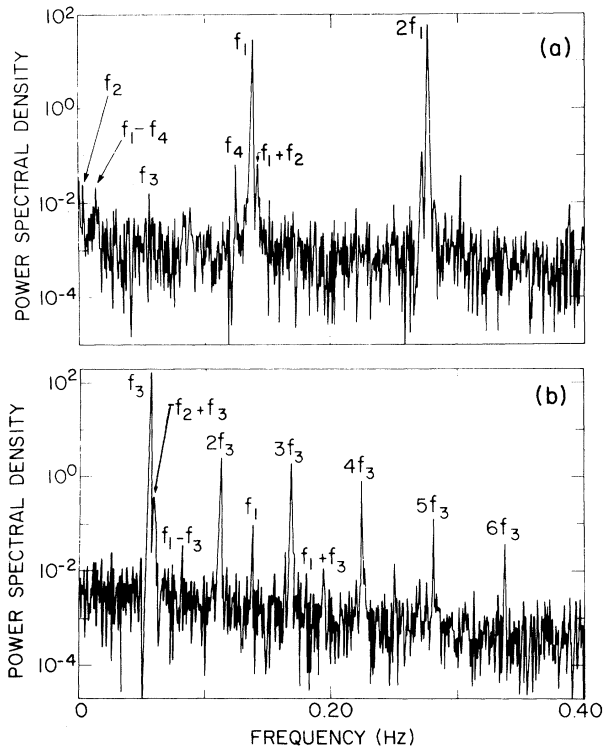

FIG. 2. Power spectra (sampling interval 0.2 s) measured at $18.7R_c$: (a) Data taken at the point marked 2(a) in Fig. 1(b); and (b) data taken at point 2(b) in Fig. 1(b).

tions of the underlying flow pattern. This tends to rule out the possibility that the location of the modes is determined by inhomogeneities in the experimental cell. The shadowgraph images indicate that the modes f_1 and f_4 (near frequencies of 137 and 124 mHz) are similar in nature with phase fronts parallel to the long side of the cell and motion of the fronts parallel to the roll axes [see Fig. 1(c)]. Motion away from the upflow boundary is also observed for f_1, but not for f_4. As shown in Fig. 1(c), mode f_3 near 55 mHz has phase fronts similar to f_1 and f_4, but it is a traveling disturbance (as opposed to a standing wave in the case of f_1 and f_4) which propagates away from the long side of the cell. The mode f_2 is qualitatively different from f_1, f_3, and f_4 having a much lower frequency of 3 mHz. As shown in Fig. 1(b), it corresponds to a "breathing" motion of the rolls. It is the only mode which has a large amplitude throughout the entire cell.

Recent calculations by Bolton, Busse, and Clever[9] provide insight into the nature of the higher-frequency modes such as f_1, f_3, and f_4. They find (for infinite aspect ratio) that several time-dependent instabilities occur in the range $R/R_c \sim 10$–15. Physically, each unstable mode corresponds to the advection of an equal number n of hot and cold "beads" or "rods" around in a roll. These modes have frequencies equal to nf_t, where f_t^{-1} is the time for the beads or rods to circulate around in a roll. For six parallel rolls in our cell, we estimate $f_t \sim 50$ mHz.[2,10] Since the observed time-dependent roll pattern is distorted from a state of parallel rolls, one might expect that modes with slightly different frequencies (e.g., f_1 and f_4) and in different parts of the cell correspond to the same value of n.

Shown in Fig. 3 are the observed frequencies as functions of R. Strong nonlinear interaction of the

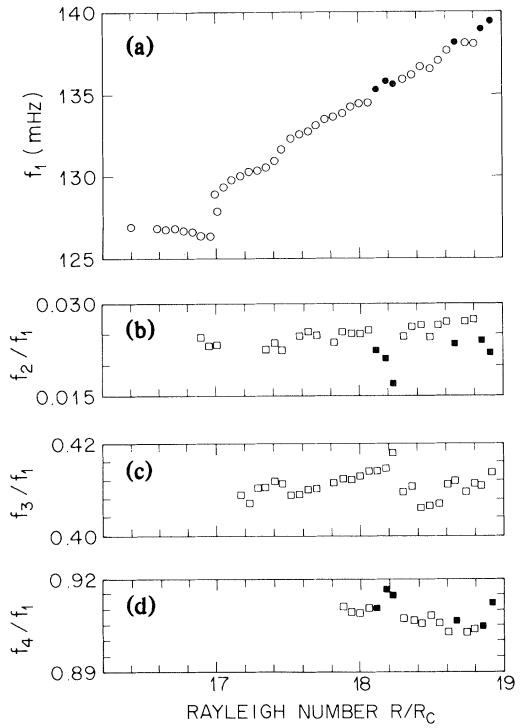

FIG. 3. The Rayleigh number dependence of (a) f_1, (b) f_2/f_1, (c) f_3/f_1, and (d) f_4/f_1. Solid symbols designate a frequency-locked state where $f_1-f_4=4f_2$.

modes is observed near $18.1R_c$; f_2 grows large in amplitude, and "locking" occurs such that $f_1-f_4-4f_2=0$. This results in only three incommensurate frequencies for $18.1<R/R_c<18.3$. Similar "locking regions" occur near $18.6R_c$ and $18.9R_c$. Above $19R_c$, the underlying six-roll flow pattern undergoes an irreversible transition to a more complex flow with a chaotic time dependence.

We have conducted several tests to show that the four modes have incommensurate frequencies and are therefore independent. Shown in Fig. 3 are f_1 and the frequency ratios f_2/f_1, f_3/f_1, and f_4/f_1, as a function of R. Each frequency is observed to have a different dependence on R. The differences between the normalized frequencies are typically much larger than the measurement errors ($\lesssim 10^{-4}$ for f_1, f_3, and f_4, and $\lesssim 10^{-2}$ for f_2). Thus, while one can find sets of integers $\{m_j\}$ such that $\sum_j m_j f_j \simeq 0$ at a particular R, no such relation holds to within our experimental error over an extended range in R.

A quantitative test for the incommensurate nature of the oscillators was obtained by a χ^2 analysis of the power spectra. The center of each line f_k was determined by linear interpolation. The error was estimated as a function peak height by use of artifical data with a noise spectrum chosen to match the experimental noise spectrum; typical errors were about 2×10^{-5} Hz. Two sets of integers $\{n_i^N\}$ were generated such that $\sum_{i=1}^{N} n_i^N f_i = f_k$ for $N=3$ and 4 incommensurate frequencies. The integers $\{n_i^N\}$ were restricted to $|n_i^N| \leq 2+m_i$, where m_i is the highest observed harmonic of the i th frequency in the spectrum. These coefficients, $\{n_i^N\}$, along with the standard deviations estimated from the peak heights, allowed calculation of χ^2 for both values of N. For two spectra at $R/R_c=18.1(18.4)$, examination of $M=23(21)$ peaks yielded $\chi^2=35.6(8.64)$ for $N=4$, and $\chi^2=2128(116)$ for $N=3$. The χ^2 values for the $N=4$ fits generally deviated from the most probable value (i.e., the number of degrees of freedom, $M-N-1$) by as much as a factor of 2, reflecting difficulty encountered[2] in estimating the error in frequency measurements by use of artificial data. However, since the addition of a redundant degree of freedom should only reduce χ^2 by about 1, these results demonstrate that the fourth frequency is necessary to explain the data satisfactorily. Varying the f_i to minimize χ^2 does not change this conclusion.

We have also studied a similar nonchaotic convecting state which exhibits five incommensurate frequencies. The basic flow pattern had six rolls which were distorted slightly differently than the pattern in Fig. 1(b). Four of these modes are spatially localized oscillations: Three of these four oscillators (observed at 123, 135, and 159 mHz) are similar in nature to the modes f_1 and f_4 described above; and the fourth, at 55 mHz, is similar to the f_3 mode of the four-frequency state. In this five-frequency state, the modes occur at different locations in the cell from those shown in Fig. 1(c). The location and nature of the fifth mode, which is observed near 6 mHz, is not known. A χ^2 analysis of the power spectra confirms that the five frequencies are incommensurate. In addition, the fractal dimension and metric entropy were calculated for this five-frequency data set. The Grassberger-Procaccia algorithm[11] gave a dimension of 5 ± 0.2; while the entropy[12] was zero within experimental error. These two numbers taken together also confirm the presence of five incommensurate frequencies without chaos.

We have presented a study of the onset of time-dependent convection in a rectangular cell of intermediate aspect ratio. The results indicate that, in contrast to observations in smaller systems, more than three modes with incommensurate frequencies can reach a finite amplitude before chaos occurs.

This study also demonstrates the importance of the spatial dependence of the mode amplitudes in determining the route to chaos in larger systems.

We wish to acknowledge the collaboration of H. Greenside on the dimension and entropy tests, conversations with E. Bolton, F. Busse, M. Cross, H. Greenside, and P. Hohenberg, and the extensive technical assistance of G. Dimino and N. Hartsough.

[1]See, for example, *Order in Chaos,* Physica (Utrecht) **7D** (1983).

[2]J. P. Gollub and S. V. Benson, J. Fluid Mech, **100**, 449 (1980).

[3]M. Gorman, L. A. Reith, and H. L. Swinney, Ann. N. Y. Acad. Sci. **357**, 10 (1980).

[4]J. Maurer and A. Libchaber, J. Phys. Lett. **41**, 515 (1980); M. Dubois and P. Bergé, Phys. Lett. **76A**, 53 (1980).

[5]C. Grebogi, E. Ott, and J. A. Yorke, Phys. Rev. Lett. **51**, 339 (1983); E. Ott, private communication; see also R. K. Tavakol and A. S. Tworkowski, Phys. Lett. **100A**, 273 (1984).

[6]Chaos is defined as an exponential divergence of nearby orbits in the phase space which describes a dynamical system; it is characterized, for example, by broad spectral components. (See Ref. 1.)

[7]F. H. Busse, and R. M. Clever, J. Fluid Mech. **91**, 319 (1979).

[8]J. P. Gollub, A. R. McCarriar, and J. F. Steinman, J. Fluid Mech. **125**, 259 (1982).

[9]E. W. Bolton, F. H. Busse, and R. M. Clever, Bull. Am. Phys. Soc. **28**, 1399 (1983); E. W. Bolton, private communication.

[10]P. Bergé, in *Chaos and Order in Nature,* edited by H. Haken (Springer-Verlag, New York, 1981), p. 14.

[11]P. Grassberger and I. Procaccia, Phys. Rev. Lett. **50**, 346 (1983), and Physica (Utrecht) **9D**, 189 (1983).

[12]Y. Termonia, Phys. Rev. A **29**, 1612 (1984).